Journal of Applied Fluid Mechanics, Vol. 12, No. 5, pp. 1629-1640, 2019.
Available online at www.jafmonline.net, ISSN 1735-3572, EISSN 1735-3645.
DOI: 10.29252/jafm.12.05.29908

Kinematics of a Cylindrical Particle at Low Reynolds Numbers in Asymmetrical Conditions

S. Champmartin[1†], A. Ambari[1] and A. Ben Richou[2]

[1] *LAMPA, Arts et Métiers ParisTech, Angers, France*
[2] *Faculty of Sciences and Technics, Sultan Moulay Slimane University, Beni-Mellal, Morocco*

†*Corresponding Author Email: stephane.champmartin@ensam.eu*

(Received December 12, 2018; accepted January 19, 2019)

ABSTRACT

This paper concerns the hydrodynamic interactions on a cylindrical particle in non-dilute regime at low Reynolds numbers. The particle moves between two parallel walls with its axis parallel to the boundaries. A numerical finite-volume procedure is implemented and a generalized resistance matrix is built by means of the superposition principle. Three problems are solved: the settling of the particle, the transport of a neutrally and of a non-neutrally buoyant particle in a Poiseuille flow. Concerning sedimentation, the settling velocity is maximal off the symmetry plane and decreases when the confinement increases. The particle rotates in the direction opposite to that of contact rolling. The particle induces a high pressure zone in the front and a low pressure zone in the back, the difference of which is maximal in the symmetry plane. For a neutrally-buoyant particle, the hydrodynamic interactions lead to a velocity lag between the particle and the undisturbed flow. The magnitude of the velocity lag increases with confinement and eccentricity. The angular velocity and pressure difference are opposite to the previous case. For a non-neutrally buoyant particle, three situations are found depending on a dimensionless parameter similar to an inverse Shields number. For its extreme low and high values, the particle is respectively either carried by the flow or settles against it whatever its position. For intermediate values, the particle either settles close to the walls or is dragged by the flow close to the symmetry plane. Similar results are obtained for the angular velocity and the pressure difference. All these results question the assumption usually met in particulate transport in which the kinematics of the particle is often supposed to be that of the flow.

Keywords: Hydrodynamic interactions; Resistance matrix; Particle transportation; Confined solid particle.

NOMENCLATURE

A_{ij}	coefficient of the resistance matrix
a	cylinder radius
b	half-distance between the walls
B_{ij}	coefficient of the resistance matrix
c	eccentricity of the particle
C_{ij}	coefficient of the resistance matrix
D_{ij}	coefficient of the resistance matrix
e	eccentricity parameter
e_{max}	maximal eccentricity parameter
F, F_i	drag force on the particle
f, g, h	generic functions
g	gravity acceleration
i, j	space index
k	confinement parameter
M, M_i	torque on the particle
R_{ij}	coefficient of the resistance matrix
U, U_i	particle velocity
U_{max}	maximal velocity of Poiseuille flow
$\bar{U}$	mean velocity of Poiseuille flow
U^*	characteristic velocity
α	ratio of gravitational to viscous forces
ΔP	pressure difference
$\Delta\rho$	density difference
μ	dynamic viscosity
ω, ω_i	angular velocity

1. INTRODUCTION

We tackle here the problem of the hydrodynamic entrainment of a cylindrical solid particle asymmetrically confined between two parallel plane walls. This kind of situations is ubiquitous in natural phenomena (sediment transport), industrial processes (settling tank, composites forming) or laboratories (separation processes in analytical chemistry such as Field-Flow Fractionation (FFF), Split-Flow Fractionation (SPLITT) or Capillary HydroDynamic Chromatography (CHDC)) among many others. In the absence of flow and for non-neutrally buoyant particles, gravity is the natural force to operate segregation and particles heavier (or lighter) than the fluid tend to segregate more rapidly. In the presence of a flow when inertia and gravity are negligible, the particles follow the direction of the streamlines with a kinematics affected by the hydrodynamic interactions. When inertia is present, lift forces appear and transverse migration across the streamlines is possible. In this work, we consider only the Stokes regimes at very low Reynolds numbers where lift forces are negligible and we want to describe the kinematics of a free cylindrical particle subject to hydrodynamic interactions from parallel boundaries. At low Reynolds numbers, these long-range interactions slowly decay (as 1/*r*) and strongly affect the motion of particles. We recall that when the particle translates in an infinite medium, the Stokes equation is not valid far from the particle: this is the famous Stokes paradox highlighted by Oseen (1910). For a cylindrical particle moving in a finite medium however, the matching of the solution at infinity is not necessary anymore and the Stokes paradox vanishes. In this case, the Stokes equation admits solutions whose properties are those of purely viscous flows: linearity, reversibility, minimum of dissipation and instantaneity (Guazzelli *et al.* (2012), Happel *et al.* (2012)) (in a previous article (Champmartin *et al.* (2007)) devoted to this kind of problems, we called "Stokes-type" the solutions having these properties). In an infinite fluid, when the particle spins on its axis, the Stokes equation do have a solution (there is no Stokes paradox for rotation). This is of course also the case in a finite medium. The articles dedicated to viscous flows around cylindrical particles confined between two parallel walls are numerous. For obvious reasons most of them propose analytical or semi-analytical solutions when the particle is symmetrically confined. In such situation, the only relevant geometrical parameter characterizing the confinement is the ratio $k = a/b$ with a the particle radius and b half the distance between the parallel walls. For a particle in uniform translation, we can quote the works of Faxén (1946), Takaisi (1955, 1956), de Mestre (1973), Katz *et al.* (1975), Tachibana *et al.* (1987), Bézine *et al.* (1981), Bouard *et al.* (1986), Bourot *et al.* (1987), Ristow (1997) or Ben Richou *et al.* (2005). All these studies propose for the drag force per unit length solutions in the following form:

$$F = 4\pi\mu U f(k) \tag{1}$$

with U the particle velocity, μ the dynamic viscosity of the fluid and $f(k)$ an increasing function in the form of a power series of k and $\ln k$. The only theoretical study about a cylindrical particle translating between parallel walls in an asymmetrical position comes from Harper *et al.* (1967) but their results are limited to very low confinements ($k < 10^{-2}$). Some numerical solutions are also available in Dvinsky *et al.* (1987a), Hu (1995) and Feng I. (1996). For a rotating cylindrical particle confined between two walls, the studies are by far less numerous and only devoted to the symmetrical problem. We can cite the papers of Howland *et al.* (1932) and Hellou *et al.* (1984, 2001). In these studies, the torque per unit length can be written in the following form:

$$M = 4\pi\mu\omega a^2 g(k) \tag{2}$$

with ω the angular velocity and $g(k)$ an increasing function of the confinement parameter. Finally, another problem often tackled is when the particle is fixed and subject to a Poiseuille plane flow. The main analytical and numerical contributions are those of Faxén (1946), Bézine *et al.* (1981), Bairstow *et al.* (1922), Takaisi (1956a,b), Harrison (1924) and Ben Richou *et al.* (2004) when the particle is in the symmetry plane. Like the case of the uniform motion of the particle, the drag force per unit length can be written as:

$$F = 4\pi\mu U_{max} h(k) \tag{3}$$

with U_{max} the maximal velocity of the Poiseuille flow and $h(k)$ an increasing function of the confinement parameter. To our knowledge, the only analytical solution for this problem when the particle is off the symmetry plane is the one of Jeong *et al.* (2014). Some numerical results are also available like those of Dvinsky *et al.* (1987b), Eklund *et al.* (1994) or Sugihara *et al.* (1984). This bibliographical review clearly reveals that most of the studies are devoted to symmetrically confined particles and that the influence of eccentricity is rarely addressed. In our previous article (Champmartin *et al.* (2007)) we studied the kinematics of a symmetrically confined free cylindrical particle for which the angular velocity is zero for obvious symmetry reasons. We solved the problems of the particle sedimentation and of its transport in a Poiseuille flow when the particle is neutrally buoyant or not. The main results of this study show that the settling velocity decreases when the confinement k increases, that a neutrally buoyant particle in Poiseuille flow lags the undisturbed flow and that a non-neutrally buoyant particle lags or leads the Poiseuille flow depending on the value of a dimensionless parameter similar to an inverse Shields number (or to the ratio of Archimedes and Reynolds numbers). In order to extend these results, we consider in this study the kinematics of a particle when it moves freely off the symmetry plane. In addition to the presence of an angular velocity, it is well established that the asymmetrical backflow in this configuration

induces a minimal drag force at an off-center position. This was clearly proved by Harper *et al.* (1967), Hu (1995), Dvinsky *et al.* (1987a,b) and Taneda (1964) for a cylindrical particle and by Brenner *et al.* (1958), Bungay *et al.* (1973) or Ambari *et al.* (1984) for a confined spherical particle.

The existence of "Stokes type" solutions for a confined cylindrical particle is a key element in this type of studies. They only exist if the particle has a finite size or moves close to an infinitely long boundary (see for example Krakowski *et al.* (1953)). When such solutions exist, it is possible to formulate the problem as a set of linear equations. A transfer matrix called here the resistance matrix can be formed whose inversion leads to the kinematics of the particle at equilibrium. Lacking in analytical solutions, the numerical approach is the most appropriate one. In this work, we numerically solved the governing equations using a finite-volume method, the details of which are reported in our previous paper (Champmartin *et al.* (2007)). The frame of this article is as follows: in section 2, the description of the problem and the resistance matrix formalism are presented. In section 3, the method is applied to solve three problems namely: the settling of the particle, its transport in a Poiseuille flow when it is neutrally and non-neutrally buoyant (particle heavier or lighter than the fluid). The first two problems (sedimentation and transport of a neutrally buoyant particle) will be compared to the few available results in order to validate our approach. Some new results concerning the influence of the particle angular velocity, the position of the maximal velocities and the pressure difference are also discussed. The last problem (transport of a non-neutrally buoyant particle) is original to our knowledge or necessitates heavy numerical procedures such as DNS. In this work, emphasis is particularly placed on the influence of the eccentricity of the particle. Finally, the last section gives the conclusion.

2. RESISTANCE MATRIX AND DESCRIPTION

As mentioned above, the formulation of the problem by a resistance matrix is related to the existence of "Stokes-type" solutions available at low Reynolds numbers in the presence of boundaries. The linearity of such solutions allows to write that at equilibrium the forces and moments are linearly coupled to the kinematics of the particle:

$$\begin{cases} F_i = \mu\left(A_{ij}U_j + B_{ij}a\omega_j\right) \\ M_i / a = \mu\left(C_{ij}U_j + D_{ij}a\omega_j\right). \end{cases} \qquad (4)$$

In the present two-dimensional problem, F_i and M_i are the force and torque components per unit length. The coefficients A_{ij} and D_{ij} relate respectively the forces to the translational velocities and the torques to the angular velocities. The coefficients B_{ij} and C_{ij} relate respectively the forces to the angular velocities and the torques to the translational velocities. The terms of this tensor have general symmetry properties from the Lorentz reciprocal theorem ($A_{ij} = D_{ij}$ and $B_{ij} = C_{ij}$). We apply this formalism in the case of a cylindrical particle of radius a confined between two parallel plane walls $2b$ apart, the particle axis remaining in the z–direction (Fig. 1). The confinement parameter $k = a/b$ varies between 0 (infinite medium) and 1 (complete blockage) and the distance c between the particle axis and the symmetry plane defines the eccentricity $e = c/b$ varying between 0 (particle in the symmetry plane) and $e_{max} = 1-k$ (particle touching one of the plane walls).

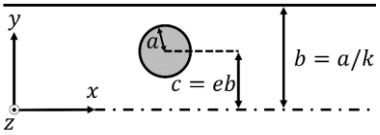

Fig. 1. Sketch of the problem.

For this two-dimensional non-inertial problem, the only existing components in (4) are the drag force F_x, the moment M_z and the velocities U_x and ω_z. We can generalize the resistance matrix by introducing the additional pressure difference ΔP induced by the motion of the particle and the mean velocity $\bar{U}$ in the presence of a plane Poiseuille flow. Using a unique notation R_{ij} for the matrix dimensionless coefficients, we obtain:

$$\begin{bmatrix} F_x \\ M_z / a \\ \Delta P\, 2b \end{bmatrix} = \mu \begin{bmatrix} R_{11} & R_{13} & R_{14} \\ R_{31} & R_{33} & R_{34} \\ R_{41} & R_{43} & R_{44} \end{bmatrix} \begin{bmatrix} U_x \\ \omega_z\, a \\ \bar{U} \end{bmatrix} \qquad (5)$$

To complete the resistance matrix, we use the superposition principle and three numerical simulations are sufficient. The details of the numerical procedure, based on a projection method and a finite volume discretization of the governing equations, are given in our previous article[4]. The first column R_{i1} is obtained by simulating a uniformly moving particle without rotation, the second column R_{i3} by simulating a uniformly rotating particle without translation and the third column R_{i4} corresponds to the simulation of a fixed particle in a plane Poiseuille flow. Figure 2 shows how the 9 R_{ij} coefficients vary as a function of the relative eccentricity e / e_{max} for the particular confinement parameter k = 0.29. The Reynolds numbers in all these simulations are very small and equal to

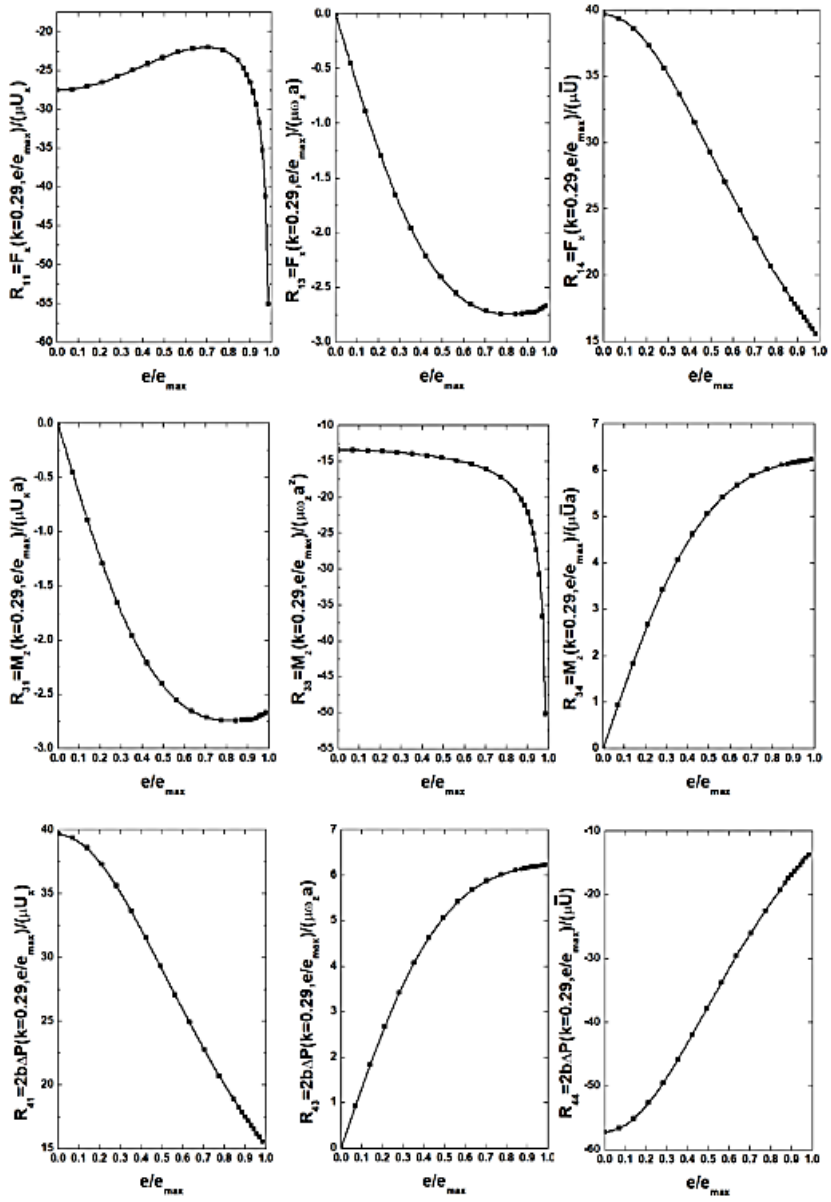

Fig. 2. $\boldsymbol{R_{ij}}$ **coefficients vs** $\boldsymbol{e}$ / $\boldsymbol{e_{max}}$ **for** $\boldsymbol{k} = 0.29$.

$\rho U_x 2a/\mu = \rho\omega_z 2a^2/\mu = \rho\bar{U}2a/\mu = 10^{-3}$ with ρ the fluid density. This ensures the existence of "Stokes type" regimes as confirmed by the equality of the extra-diagonal terms of the resistance matrix visible in Fig. 2. Once the matrix is complete, it is possible to use it to solve the kinematics of a freely moving particle at equilibrium. Three situations are considered: a particle settling along the plane walls, a neutrally buoyant particle transported by a plane Poiseuille flow and finally a non-neutrally buoyant particle transported by a plane Poiseuille flow.

3. RESULTS AND DISCUSSION

3.1 Particle Sedimentation

The first problem we can solve is the settling of the particle when gravity acts parallelly to the walls. At equilibrium when the particle reaches its terminal velocities, the apparent weight exactly equals the drag force and the torque on the particle is zero. The linear system to solve is therefore:

$$\begin{bmatrix} -\Delta\rho g\,\pi a^2 \\ 0 \\ \Delta P\,2b \end{bmatrix} = \mu \begin{bmatrix} R_{11} & R_{13} & R_{14} \\ R_{31} & R_{33} & R_{34} \\ R_{41} & R_{43} & R_{44} \end{bmatrix} \begin{bmatrix} U_x \\ \omega_z a \\ 0 \end{bmatrix} \tag{6}$$

with $\Delta\rho$ the density difference between the particle and the fluid. The settling velocity can be written as:

$$U_x = \left(\frac{-R_{33}}{R_{11}R_{33} - R_{13}R_{31}}\right) U^* \tag{7}$$

xwith $U^* = \Delta\rho g\,\pi a^2/\mu$ a characteristic velocity. In Fig. 3 we have plotted the evolution of

U_x/U^* as a function of e/e_{max} for three confinement parameters k. The numerical results from the article of Dvinsky *et al.* (1987a) for $k=0.5$ and $k=0.6$ are also given and agree well with ours.

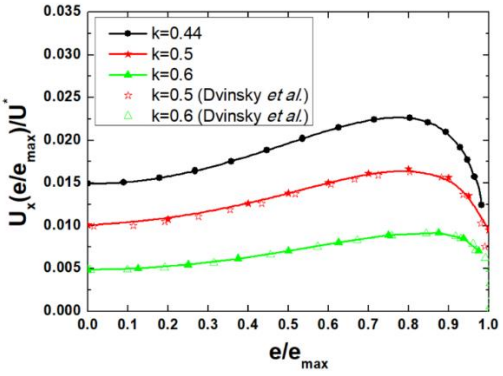

Fig. 3. Dimensionless settling velocity vs e/e_{max} for $k=0.44$, $k=0.5$ and $k=0.6$.

These curves show that the settling velocity decreases when k increases and evidence the growing effect of the hydrodynamic interactions as the confinement increases. The backflow induced by the sedimenting particle is more and more confined when k increases and enhances the drag force on the particle. This phenomenon was accurately quantified in our previous article (Champmartin *et al.* (2007)) for the particular symmetrical position (in that case $R_{13}=R_{31}=0$ and the settling velocity (Eq.7) depends only on the drag force coefficient R_{11}). Figure 3 also reveals that for a given confinement, the maximal settling velocity is off the symmetry position. This effect is also related to the drag force on the particle which is minimum at an off-center position as it is visible in Fig. 2 with the R_{11} coefficient of the resistance matrix. At this particular position, even if the coefficients $R_{13}=R_{31}$ are not zero, the analysis of these terms in Eq.7 shows that they are one order of magnitude lower than the terms R_{11} and R_{33}. Consequently the settling velocity is only weakly affected by the particle angular velocity and behaves closely as $U_x \approx -1/R_{11}$. This result is also observed in Harper *et al.* (1967), Dvinsky *et al.* (1987a), Hu (1995), Feng *et al.* (1996) and Taneda (1964) and in the analogous problem of a spherical particle confined in a cylindrical tank in Brenner *et al.* (1958), Bungay *et al.* (1973) or Ambari *et al.* (1984). The local off-center minimum of the drag force comes from the asymmetrical distribution of the backflow in such confined media (this phenomenon disappears for a spherical particle settling between two infinite parallel walls where the backflow is not confined anymore).

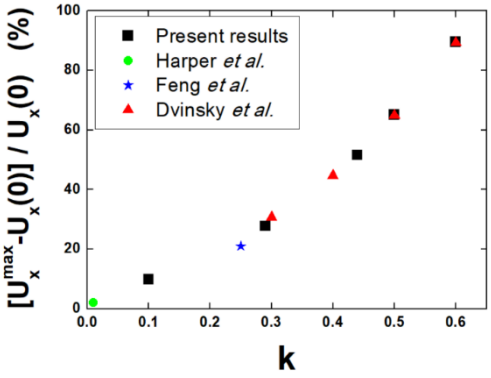

Fig. 4. Relative maximal increase in the settling velocity vs k.

In Fig. 4, we plot as a function of k the relative maximal increase in the settling velocity compared to its value in the symmetrical position. Our numerical results are in accordance with those of Harper *et al.* (1967), Dvinsky *et al.* (1987a) and Feng *et al.* (1996). The relative augmentation is an increasing function of the confinement and seems to increase non-linearly. The more confined the particle, the slower its settles and the more its velocity is sensitive to position. The angular velocity of the settling particle is:

$$\omega_z = \left(\frac{R_{31}}{R_{11}R_{33}-R_{13}R_{31}}\right)\frac{U^*}{a} \qquad (8)$$

It is plotted in Fig. 5 for three confinement parameters. This velocity was also calculated by Dvinsky *et al.* (1987a) and their results are in qualitative agreement with ours.

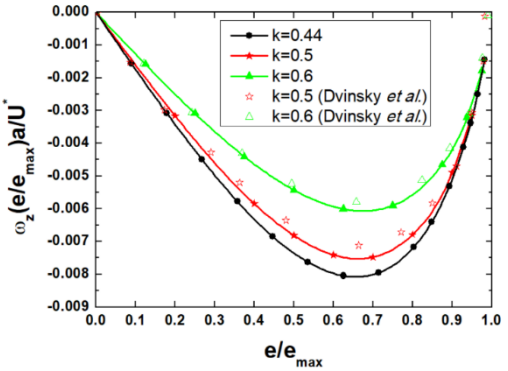

Fig. 5. Dimensionless angular velocity vs e/e_{max} for $k=0.44$, $k=0.5$ and $k=0.6$.

From symmetry, $\omega_z=0$ in the mid-plane. Like the settling velocity, the hydrodynamic interactions impede all the more the rotation of the particle when k increases. As the eccentricity increases, the magnitude of the angular velocity increases, reaches a maximum and finally steeply decreases when $e/e_{max} \to 1$. In lubrication regime, the asymptotical behaviors of the R_{ij} coefficients

indicate that the rotation of the particle vanishes when it touches the wall. Figure 6 displays the relative positions $(e/e_{max})^{\omega_z^{max}}$ and $(e/e_{max})^{U_x^{max}}$ at which the amplitude of the angular and settling velocities are maximal. When the confinement increases, the position of the maximal velocities moves away from the symmetry plane but U_x and ω_z are not maximal at the same position. The evolutions seem to be linear at least in the present range $k<0.7$. At low confinements for $k<0.17$, the settling velocity reaches its maximum closer to the symmetry plane than the angular velocity and for $k>0.17$, the angular velocity is maximum closer to the symmetry plane than the settling velocity.

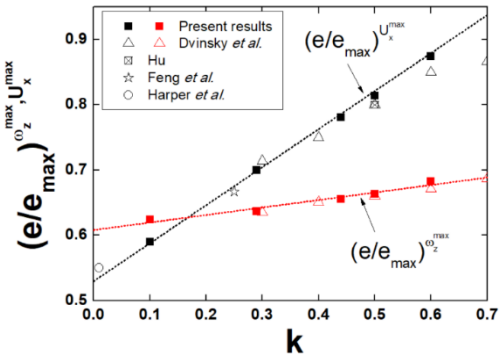

Fig. 6. Relative position of the maximal settling and angular velocities vs k .

Some data from the studies of Harper *et al.* (1967), Dvinsky *et al.* (1987a), Hu (1995) and Feng *et al.* (1996) are also reported in this figure and agree well with our results. A noteworthy characteristic of the angular velocity is its sense of rotation: the negative sign of ω_z in Fig. 5 indicates that the particle rotates in the direction opposite to that of contact rolling with the nearby wall. The word "anomalous rolling" is sometimes found in the bibliography (Hu (1995) or Liu *et al.* (1993)). To explain this sense of rotation, Fig. 7 shows the streamlines around the particle in a reference frame translating at the settling velocity U_x for $k=0.5$ and $e/e_{max}=0.5$.

We observe that the flow between the particle and the plane nearby is very weak and that most of the fluid bypasses the particle from below inducing the apparently "anomalous" sense of rotation. In his article, Hu (1995) thoroughly analyzed the stress distribution on the particle to confirm this phenomenon. Dvinsky *et al.* (1987a) claim however that in the very vicinity of the wall, the particle changes its sense of rotation (like it is proven for a spherical particle settling in a cylindrical tank) but their result is in contradiction with the evolution of the torque they calculate (Fig. 4 in their article) because it monotonically tends to infinity without changing its sign. The accuracy of their numerical results in this lubrication regime is probably questionable. When the particle settles, it produces in the surrounding fluid a disturbance in the pressure field: the pressure is higher in front of the particle and lower behind. The resistance matrix can calculate this pressure difference:

$$\Delta P=\left(\frac{R_{43}R_{31}-R_{41}R_{33}}{R_{11}R_{33}-R_{13}R_{31}}\right)\frac{\mu U^*}{2b} \qquad (9)$$

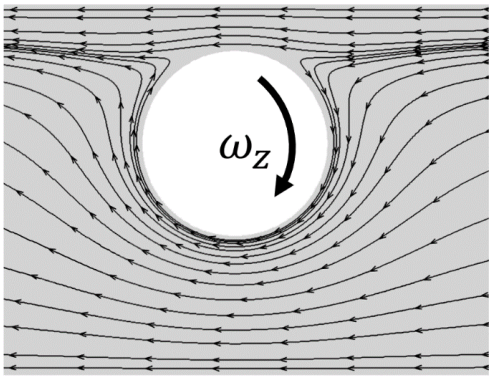

Fig. 7. Streamlines around the settling particle ($k=e/e_{max}=0.5$).

Figure 8 shows the dimensionless pressure difference for three confinement parameters. It is maximal in the symmetry plane and monotonically decreases when the particle gets closer to a wall. The numerical results of Dvinsky *et al.* (1987a) are also plotted and accord reasonably well with ours. At first glance, it seems in Fig. 8 that at low eccentricities the pressure difference varies as the inverse of the confinement parameter (the smaller the particle, the larger the pressure difference). This misleading analysis is due to the scales used to adimensionnalize the pressure difference which depend on *a* and *b*. In fact, in a given fluid, a particle produces a pressure difference that increases as the confinement increases whatever its position in the channel. In Fig. 9 the individual contributions to ΔP of translation and rotation are plotted for $k=0.5$. We notice that the translational motion of the particle results in a positive pressure difference whereas the rotational motion of the particle induces a negative pressure difference because of its "anomalous" sense. The former being one order of magnitude greater than the latter, the total pressure difference remains positive. We see again that rotation weakly affects the results (for $k=0.6$ if we constrain the particle to settle without rotation, both U_x and ΔP change at most by 5% at the position where ω_z is maximum).

3.2 Neutrally Buoyant Particle in Poiseuille flow

The second problem we can solve is the transport of the particle in a plane Poiseuille flow with average velocity $\bar{U}$ when the densities of the particle and of the fluid match ($\Delta\rho=0$). In that case, both the forces and torques on the particle are zero and the resistance matrix formalism is:

$$\begin{bmatrix} 0 \\ 0 \\ \Delta P\, 2b \end{bmatrix} = \mu \begin{bmatrix} R_{11} & R_{13} & R_{14} \\ R_{31} & R_{33} & R_{34} \\ R_{41} & R_{43} & R_{44} \end{bmatrix} \begin{bmatrix} U_x \\ \omega_z a \\ \bar{U} \end{bmatrix} \tag{10}$$

The transport velocity is then:

$$U_x = \left(\frac{R_{13}R_{34} - R_{14}R_{33}}{R_{11}R_{33} - R_{13}R_{31}} \right) \bar{U} \tag{11}$$

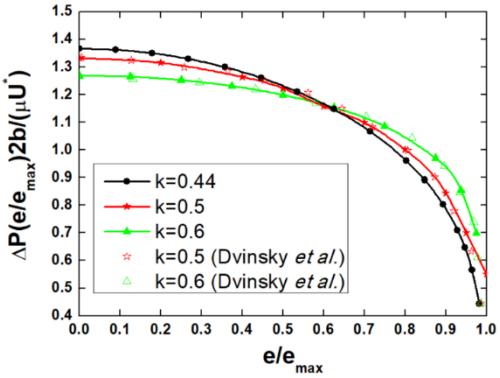

Fig. 8. Pressure difference around the settling particle vs e/e_{max}.

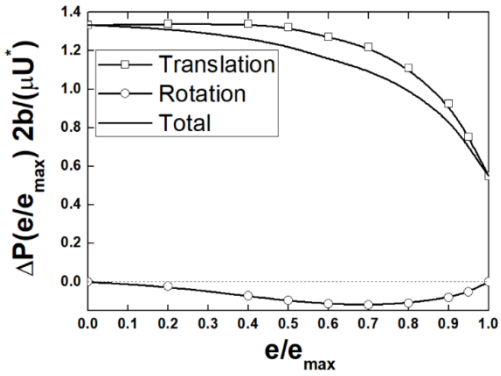

Fig. 9. Pressure difference due to translation and rotation for $k = 0.5$ vs e/e_{max}.

Figure 10 shows how the dimensionless transport velocity $U_x/\bar{U}$ varies according to e/e_{max} for three confinements. Some results from the articles of Jeong *et al.* (2014) (for $k = 0.5$ and $k = 0.6$), Dvinsky *et al.* (1987b) (for $k = 0.5$ and $k = 0.6$) and Eklund *et al.* (1994) (for $k = 0.5$) are also reported in Fig. 10 and agree qualitatively well with ours.

For a given k value, this velocity is maximal in the symmetry plane and monotonically decreases when the eccentricity increases. Logically the particle transport velocity follows the same trend as the Poiseuille flow. According to the asymptotic behaviors of the R_{ij} coefficients, U_x vanishes when $e/e_{max} \to 1$. In the same figure, the dotted lines represent for each k value the velocity profile of the undisturbed plane Poiseuille flow. It is clear that a neutrally buoyant particle lags the flow and that the velocity lag enhances as confinement and eccentricity increase. In particular in the symmetry plane ($e/e_{max} = 0$) we can use some results from our previous article (Champmartin *et al.* (2007)) to calculate the relative lag velocity:

$$\frac{U_{max} - U_x\left(e/e_{max} = 0\right)}{\bar{U}} = \frac{3k^2}{4 + 2k^2} \tag{12}$$

In the limit $k \to 0$, the particle translates at the fluid velocity U_{max}. In this limit, Eq.12 also agrees with Faxén's law (Faxén, 1922) for a spherical particle which states that the particle lags the fluid with a difference of the order of k^2. In their article, Dvinsky *et al.* (1987b) proposed the expression:

$$\frac{U_{max} - U_x\left(e/e_{max} = 0\right)}{\bar{U}} = \frac{3k^{\gamma}}{2^{\gamma+1} + 2k^{\gamma}} \tag{13}$$

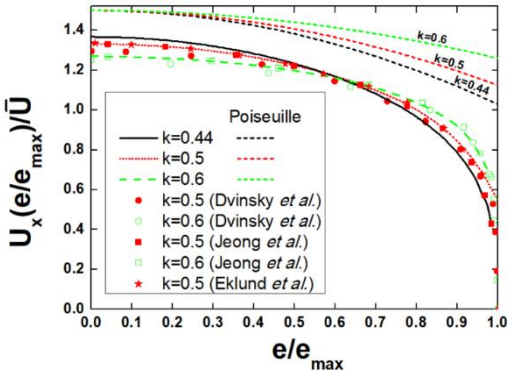

Fig. 10. Transport velocity of a neutrally buoyant particle in a plane Poiseuille flow vs e/e_{max}.

with $\gamma = 1.91$ obtained from a fitting of their numerical results. Although Eq.12 and Eq.13 give similar results in the limit of low confinements, both rapidly diverge when k increases. The numerical results of Dvinsky *et al.* (1987b) are again doubtful at high confinements. Indeed in the lubrication regime when $k \to 1$, Eq.12 shows that $U_x\left(e/e_{max} = 0\right) \to \bar{U}$ that is, to say, that the particle behaves like a plug moving at the mean velocity $\bar{U}$ whereas Eq.13 gives $U_x\left(e/e_{max} = 0\right) \to 1.2395\,\bar{U}$. Moreover the analytical results of Jeong *et al.* (2014) match accurately those given by Eq.12 (within 0.12% relative error). The angular velocity of the particle writes:

$$\omega_z = \left(\frac{R_{31}R_{14} - R_{11}R_{34}}{R_{11}R_{33} - R_{13}R_{31}} \right) \frac{\bar{U}}{a} \tag{14}$$

It is plotted in Fig. 11 for three confinement parameter as a function of e/e_{max}. Some results from the articles of Jeong *et al.* (2014) (for $k=0.5$ and $k=0.6$), Dvinsky *et al.* (1987b) (for $k=0.5$ and $k=0.6$) and Eklund *et al.* (1994) (for $k=0.5$) are also reported in Fig.11 and agree qualitatively well with ours. The rotation is zero in the midplane as expected from symmetry, it increases when e/e_{max} increases, reaches a local maximum and finally steeply decreases when $e/e_{max}\to 1$. The asymptotic behaviors of the coefficients R_{ij} indicate that ω_z vanishes when the particle touches one of the plane walls. In the same figure the dotted lines give the local vorticity of the undisturbed Poiseuille flow:

$$\omega_z = \frac{3}{2}k(1-k)\frac{e}{e_{max}}\frac{\bar{U}}{a} \tag{15}$$

According to Faxén's law (Faxén, 1922), the solid particle should rotate at the same angular velocity as the fluid. This is clearly in contradiction with the results in Fig. 11 in which the angular velocity of the cylindrical particle is always lower than that of the fluid. The angular velocity lag increases when both k and e/e_{max} increase like in the case of the transport velocity U_x. Contrary to sedimentation, the angular velocity of the neutrally buoyant particle is positive and the "anomalous rolling" phenomenon has disappeared.

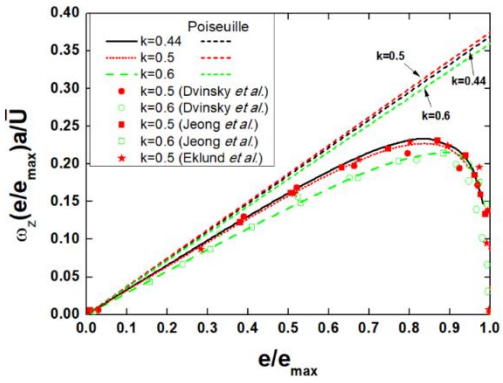

Fig. 11. Angular velocity of a neutrally buoyant particle in a plane Poiseuille flow vs e/e_{max}.

In Fig. 12 we can see the streamlines around the particle for $k=e/e_{max}=0.5$ in a reference frame moving at the transport velocity U_x. We notice the existence of "Stokes cells" appearing because of the coupling between the shear in the Poiseuille flow and the backflow induced by the particle movement. Like for the settling problem, the "weak" backflow due to the particle motion in the region above the particle induces an anti-clockwise sense of rotation and the "strong" backflow in the region below the particle induces a clockwise sense of rotation but due to the velocity gradient of the Poiseuille flow, this latter effect is counterbalanced by the velocity of the Poiseuille flow which is stronger below the particle. As a consequence, all the particle surface is subject to an anticlockwise flow and the particle rotates as if rolling along the plane nearby. The additional pressure change due to the cylindrical particle is:

$$\Delta P = \left\{ \frac{R_{41}(R_{13}R_{34}-R_{14}R_{33})}{R_{11}R_{33}-R_{13}R_{31}} + \frac{R_{43}(R_{31}R_{14}-R_{11}R_{34})}{R_{11}R_{33}-R_{13}R_{31}} + R_{44} \right\} \frac{\mu\bar{U}}{2b} \tag{16}$$

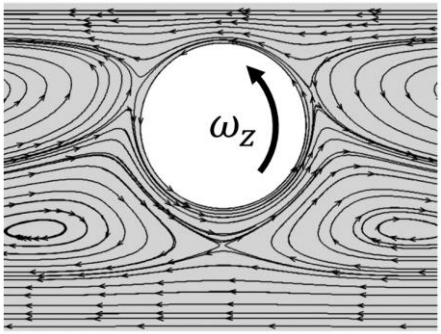

Fig. 12. Streamlines around the transported particle in a plane Poiseuille flow ($k=e/e_{max}=0.5$).

It is plotted in Fig. 13 for three confinement parameters. Some results from the articles of Jeong *et al.* (2014) (for $k=0.5$ and $k=0.6$), Dvinsky *et al.* (1987b) (for $k=0.5$ and $k=0.6$) are also plotted and agree well with our data.

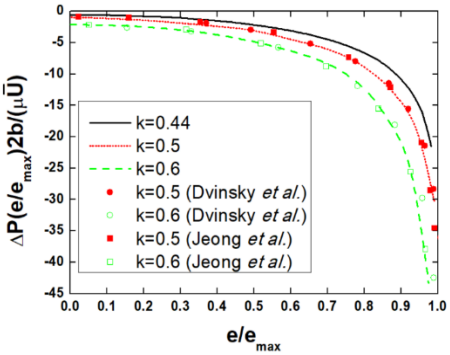

Fig. 13. Pressure difference induced by the transported particle in a plane Poiseuille flow vs e/e_{max}.

The negative sign of ΔP indicates that the particle produces an additional pressure loss. The magnitude of ΔP is minimal in the symmetrical position and increases monotonically when the eccentricity and the confinement increase. The three terms in Eq.16 represent from left to right the pressure difference due to the translational motion, the rotational motion and the Poiseuille flow. These

individual contributions are plotted in Fig. 14. We notice that ΔP induced by the particle translation (square symbols) and rotation (star symbols) are positive whereas ΔP due to Poiseuille flow (circle symbols) is negative. The contribution of rotation is again very small compared to the others and the total ΔP is mainly due to the competition between the positive contribution of translation and the negative contribution of Poiseuille flow, this latter dominating the former at every position. Another interesting result is that the magnitude of the pressure loss for a fixed particle (circle symbols) is much larger than the pressure loss for a free particle (solid line) and that their dependence on e/e_{max} is opposite.

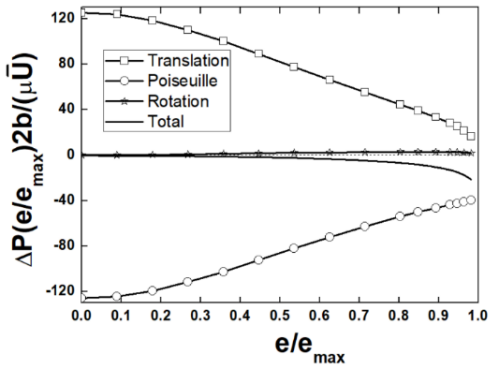

Fig. 14. Pressure difference induced by translation, rotation and Poiseuille flow vs e/e_{max} for $k=0.5$.

3.3 Non-Neutrally Buoyant Particle in Poiseuille flow

The last problem we can look at is when the particle is non-neutrally buoyant ($\Delta\rho \neq 0$). To our knowledge, this is the first attempt to solve such a problem in the Stokes regime limit with the resistance matrix approach although in actual particulate transport problems, the fluid and particle densities rarely match. In virtue of the linearity of the equations and of the boundary conditions, this problem can be solved using the superposition principle. Let us suppose that gravity acts in the opposite direction as the Poiseuille flow. The transport velocity of the free particle now writes:

$$U_x = \left\{ \frac{R_{13}R_{34} - R_{14}R_{33}}{R_{11}R_{33} - R_{13}R_{31}} + \alpha \frac{R_{33}}{R_{11}R_{33} - R_{13}R_{31}} \right\} \bar{U} \tag{17}$$

with $\alpha = U^*/\bar{U}$ ($\alpha > 0$ when the particle density is larger than the density of the fluid). This parameter is the ratio of gravitational to viscous forces (it can be seen as the inverse of the Shields number used in sediment transport). In Fig.15 we can see the transport velocity (Eq.17) as a function of e/e_{max} for the particular confinement parameter $k = 0.29$ and various values of α.

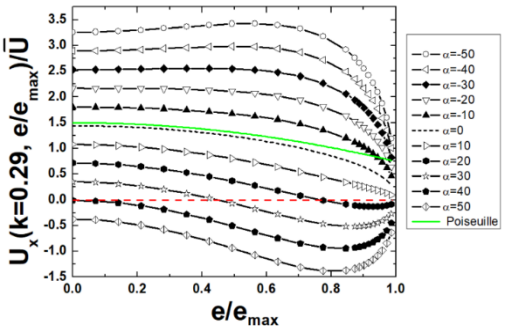

Fig. 15. Transport velocity of a non-neutrally buoyant free particle in a plane Poiseuille flow vs e/e_{max} for $k=0.29$.

For $\alpha > 40$, the transport velocity in negative at every transverse position and the particle always settles against the Poiseuille flow. The velocity profile is non-monotonous with the same trend as the settling velocity in Fig. 3. For $15 < \alpha < 40$, the sign of U_x depends on the position of the particle in the channel: if it is close to the symmetry plane, it is transported by the Poiseuille flow and if the particle is close to a plane wall, it settles in the reverse direction. In the range $15 < \alpha < 40$, the evolution of U_x is still non-monotonous but the position of the negative minimal velocity shifts toward the plane nearby when α decreases (increasing influence of the Poiseuille flow). When $0 < \alpha < 15$, the transport velocity of the particle becomes positive regardless of its position and the particle always moves in the same direction as the Poiseuille flow. The velocity is maximal in the symmetry plane and decreases monotonically when e/e_{max} increases. We notice also that the particle lags the fluid (the Poiseuille velocity profile is plotted in green solid line in Fig. 15). When $\alpha < 0$, the particle is "lighter" than the fluid and sedimentation turns into flotation. In that case, the transport velocity of the Poiseuille flow adds to the flotation velocity and the particle can lead the fluid. Finally for $\alpha < -20$, the transport velocity profile becomes again non-monotonous showing the dominating effect of the flotation velocity compared to the transport velocity of the Poiseuille flow. In Fig.16, we can see the evolution of the angular velocity as a function of e/e_{max} for various values of α and for $k = 0.29$. The expressions of ω_z can be easily obtained by adding the respective contributions of the sedimentation and of the neutrally buoyant particle problems:

$$\omega_z = \left\{ \frac{R_{31}R_{14} - R_{11}R_{34}}{R_{11}R_{33} - R_{13}R_{31}} - \alpha \frac{R_{31}}{R_{11}R_{33} - R_{13}R_{31}} \right\} \frac{\bar{U}}{a} \tag{18}$$

This figure shows that the angular velocity can be either positive throughout the channel, negative throughout the channel or change its sign depending on its position. For this particular confinement parameter $k = 0.29$, the angular velocity is always positive when $\alpha > -17$ and always negative when

$\alpha < -113$. In the range $-113 < \alpha < -17$, the angular velocity is negative from the symmetry plane up to a transverse position that shifts towards the plane wall as α decreases. For $\alpha > 0$, we notice that the particle can rotate faster than the undisturbed fluid particle (the green solid line in Fig. 16) with the same sense of rotation. The critical values of α separating the transport ($U_x > 0$) and sedimentation ($U_x < 0$) regimes and the $\omega_z > 0$ and $\omega_z < 0$ rotation regimes are obtained from Eq.17 and Eq.18 by solving $U_x = 0$ and $\omega_z = 0$. For the translational motion, we obtain:

$$\alpha_c = R_{14} - \frac{R_{13}R_{34}}{R_{33}} \tag{19}$$

For the rotational motion, we obtain:

$$\alpha_c = R_{14} - \frac{R_{11}R_{34}}{R_{31}} \tag{20}$$

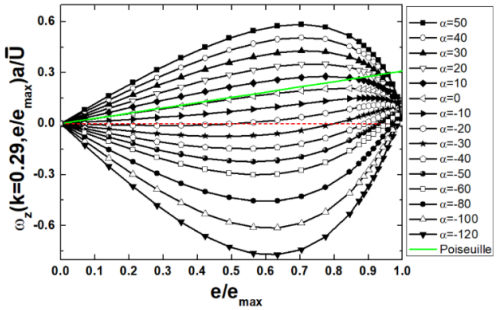

Fig. 16. Angular velocity of a non-neutrally buoyant free particle in a plane Poiseuille flow vs e/e_{max} for $k = 0.29$.

These critical parameters are plotted in Fig.17. They define three regions and three kinematics for the particle depending on α and on its eccentricity.

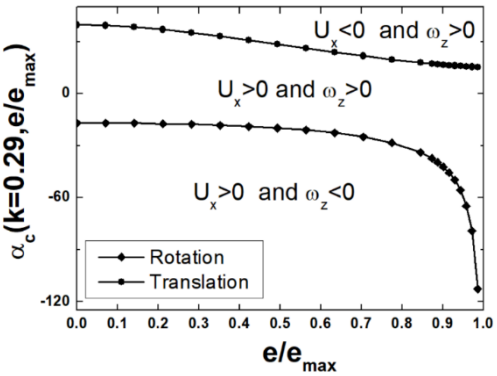

Fig. 17. Critical values of α for the translational and angular velocities of a non-neutrally buoyant free particle in a plane Poiseuille flow vs e/e_{max} for $k = 0.29$.

In the case of separation processes usually used in analytical chemistry, the particular regime for which the particle is either transported or settles depending on its position can play an important role. The lower bound α_{min} and upper bound α_{max} defining this regime depend obviously on the confinement. We have plotted these limits in Fig. 18 as a function of k. If $\alpha < \alpha_{min}(k)$, the particle always moves in the same direction as the Poiseuille flow. If $\alpha > \alpha_{max}(k)$ the particle always settles in the inverse direction of the Poiseuille flow. If $\alpha_{min}(k) < \alpha < \alpha_{max}(k)$ the sign of U_x depends on the particle position.

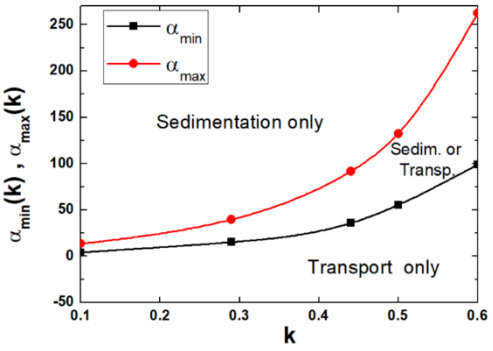

Fig. 18. Values of α_{min} and α_{max} for U_x vs k.

Finally, the pressure difference induced by the particle is obtained by combining Eq.9 and Eq.16. We consider here the pressure difference between two sections placed respectively above and below the particle (the pressure difference due to the Poiseuille flow is always negative and the pressure difference due to settling or floating is positive or negative depending on a and on the particle position). The total pressure difference is plotted in Fig. 19 for $k = 0.29$ and various values of α.

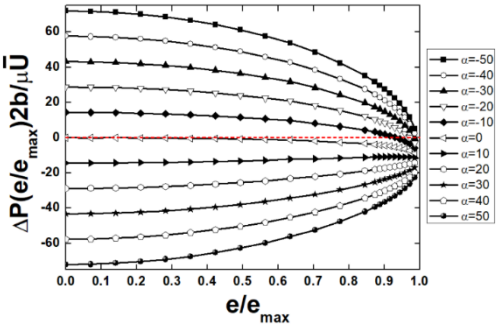

Fig. 19. Pressure difference for a non-neutrally buoyant free particle in a plane Poiseuille flow for $k = 0.29$ vs e/e_{max}.

Qualitatively this figure shows that the pressure difference is positive when $\alpha < 0$ and inversely except in the very vicinity of the plane wall. If we look at Fig. 8 and Fig. 13, we notice that when the particle is close to a plane wall, the pressure difference due to the sedimentation or flotation is very small compared to that of the Poiseuille flow. Consequently, all the curves in Fig. 19 seem to converge towards the same negative value

corresponding to the pressure difference of the Poiseuille flow alone when $e/e_{max} \to 1$. In the opposite limit when $e/e_{max} \to 0$, most of the pressure difference comes from the sedimentation/flotation phenomenon. When $\alpha > 0$, the pressure difference due to sedimentation is negative and adds to the negative pressure difference of the Poiseuille flow. When α increases, this effect is enhanced and the pressure difference becomes more and more negative. When $\alpha < 0$, the pressure difference due to flotation is positive. When *a* decreases, the negative pressure difference due to the Poiseuille flow is rapidly compensated and overcome, leading to an increasing positive pressure difference.

4. CONCLUSION

We took advantage of the mathematical properties of the "Stokes-type" solutions at low Reynolds numbers to solve the kinematics of a free cylindrical particle in asymmetrical position between two parallel plane walls. Three problems were tackled using a finite volume numerical approach and a projection method enabling to compute the terms of the generalized resistance matrix: the first problem is the settling of the particle parallelly to the walls. The hydrodynamic interactions lead to a maximal settling velocity off the symmetry plane. The relative position of the extremal settling and angular velocities are linearly related to the confinement parameter. The sense of rotation of the particle is opposite to contact rolling with the plane nearby and the motion of the particle induces a positive pressure difference between two sections placed in front and behind the particle respectively. The second problem concerns the transport of a neutrally buoyant particle in a plane Poiseuille flow. The transport velocity is maximal in the symmetry plane and follows the same trend as the undisturbed Poiseuille profile. The sense of rotation of the particle is opposite to that of sedimentation. For the translational and angular velocities, the solid particle always lags the undisturbed fluid particle at the same position. This effect is enhanced when the confinement and the eccentricity of the particle increase. The pressure difference induced by the particle motion is negative. The last problem is the transport of a non-neutrally buoyant particle in a plane Poiseuille flow. The particle can be heavier or lighter than the surrounding fluid. Several possible kinematics are found depending on the value of a control parameter defined as the ratio of the gravitational force to the viscous force. Three regimes were identified: whatever its position in the channel, the particle can settle against the Poiseuille flow or be transported by it. In the third regime, the particle direction depends on its position: close to the symmetry plane, the particle is transported by the Poiseuille flow and close to the plane wall the particle settles in the opposite direction. The control parameter also dictates the sense of rotation of the particle and the pressure difference due to its motion. From a general point of view, the rotation of the particle plays a minor role in its translational velocity and disturbs weakly the pressure field around the particle. These results highlight the role of the hydrodynamic interactions at low Reynolds numbers in the transport of solid particles in non-dilute regimes at high confinements and eccentricities. They could be useful in the numerical modeling of fiber transport or in the design of separation devices commonly used in analytical chemistry. Let us note that the present technique can be easily generalized if the particle undergoes other external forces such as electric or magnetic forces.

REFERENCES

Ambari, A., B. Gauthier-Manuel and E. Guyon (1984). Wall effects on a sphere translating at constant velocity. *Journal of Fluid Mechanics* (149), 235-253.

Bairstow, L., B.M. Cave and E.D. Lang (1922). The two-dimensional slow motion of viscous fluids. *Proceedings of the Royal Society of London* (100), 394-413.

Ben Richou, A., A. Ambari and J. K. Naciri (2004). Drag force on a circular cylinder midway between two parallel plates at very low Reynolds number. Part 1: Poiseuille flow (numerical). *Chemical Engineering Science* (59), 3215-3222.

Ben Richou, A., A. Ambari, M. Lebey and J. K. Naciri (2005). Drag force on a circular cylinder midway between two parallel plates at Re<<1. Part 2: moving uniformly (numerical and experimental). *Chemical Engineering Science* (60), 2535-2543.

Bézine, G. and D. Bonneau (1981). Integral equation method for the study of two dimensional Stokes flow. *Acta Mechanica* (41), 197-209.

Bouard, R. and M. Coutanceau (1986). Etude théorique et expérimentale de l'écoulement engendré par un cylindre en translation uniforme dans un fluide visqueux en régime de Stokes. *Z. Angew. Math. Phys.* (37), 673-684.

Bourot, J. M. and F. Moreau (1987). Sur l'utilisation de la série cellulaire pour le calcul d'écoulements plans de Stokes en canal indéfini. *Mechanics Research Communications* (14), 187-197.

Brenner, H. and J. Happel (1958). Slow viscous flow past a sphere in a cylindrical tube. *Journal of Fluid Mechanics* (4), 195-213.

Bungay, P. M. and H. Brenner (1973). The motion of a closely-fitting sphere in a fluid-filled tube. *International Journal of Multiphase Flow* (1), 25-56.

Champmartin, S. and A. Ambari (2007). Kinematics of a symmetrically confined cylindrical particle in a "Stokes-type" regime. *Physics Fluids* (19), 073303.

De Mestre, N. J. (1973). Low-Reynolds-number fall of slender cylinders near boundaries. *Journal of*

Fluid Mechanics (58), 641-656.

Dvinsky, A. S. and A. S. Popel (1987a). Motion of a rigid cylinder between parallel plates in a Stokes flow. Part 1: motion in a quiescent fluid and sedimentation. *Computers & Fluids* (15), 391-404.

Dvinsky, A. S. and A. S. Popel (1987b). Motion of a rigid cylinder between parallel plates in a Stokes flow. Part 2: Poiseuille and Couette flow. *Computers & Fluids* (15), 405-419.

Eklund, E. and A. Jernqvist (1994). The motion of a neutrally buoyant circular cylinder in bounded shear flows. *Chemical Engineering Science* (49), 3765-3772.

Faxén, H. (1922). Der Widerstand gegen die Bewegung einer starren Kugel in einer zähen Flüssigkeit, die zwischen zwei parallelen ebenen Wänden eingeschlossen ist. *Annals of Physics (*373), 89-119.

Faxén, H. (1946). Forces exerted on a rigid cylinder in a viscous fluid between two parallel fixed planes. *in Proceedings of the Royal Swedish Academy of Engineering Science* (187),1-13.

Feng, J., P. Y. Huang and D. D. Joseph (1996). Dynamics simulation of sedimentation of solid particles in an Oldroyd-B fluid. *Journal of Non-Newtonian Fluid Mechanics*(63), 63-88.

Guazzelli, E. and J. F. Morris (2012). *A Physical Introduction to Suspension Dynamics*, Cambridge University Press.

Happel, J. and H. Brenner (2012). *Low Reynolds number hydrodynamics: with special applications to particulate media (Vol. 1)*, Springer Science & Business Media.

Harper, E. Y. and I. D. Chang (1967). Drag on a cylinder between parallel walls in Stokes' flow. *Physics Fluids* (10), 83-88.

Harrison, W. J. (1924). On the motion of spheres, circular and elliptic cylinders through viscous liquid. *Transactions of the Cambridge Philosophical Society* (23), 10-88.

Hellou, M. and M. Coutanceau (1992). Cellular Stokes flow induced by rotation of a cylinder in a closed channel. *Journal of Fluid Mechanics* (236), 557-577.

Hellou, M. (1984). *Etude numérique et expérimentale de l'écoulement à structure cellulaire, engendré par la rotation d'un cylindre dans un canal*, Ph. D. thesis, University of Poitiers, France.

Hellou, M. (2001). Sensitivity of cellular Stokes flow to geometry. *European Journal of Physics* (22), 67.

Howland, R. C. J. (1932). Slow rotation of a circular cylinder in a viscous fluid bounded by parallel walls. *in Proceedings of the Cambridge Philosophical Society* (29), 277-287.

Hu, H. H. (1995). Motion of a circular cylinder in a viscous liquid between parallel plates. *Theoretical and Computational Fluid Dynamics* (7), 441-455.

Jeong, J. T. and C. S. Jang (2014). Slow motion of a circular cylinder in a plane Poiseuille flow in a microchannel. *Physics Fluids* (26), 123104.

Katz, D. F., J. R. Blake and S. L. Paveri-Fontana (1975). On the movement of slender bodies near plane boundaries at low Reynolds number. *Journal of Fluid Mechanics* (72), 529-540.

Krakowski, M. and A. Charnes (1953). Stokes paradox and biharmonic flows. *Carnegie Institute of Technology, Report N°37.*

Liu, Y. J., J. Nelson, J. Feng and D. D. Joseph (1993). Anomalous rolling of spheres down an inclined plane. *Journal of Non-Newtonian Fluid Mech.* (50), 305-329.

Oseen, C. W. (1910). Über die Stokessche Formel und über eine verwandte Aufgabe in der Hydrodynamik. *Arkiv för matematik, astronomi och fysik* (6), 1.

Ristow, H. G. (1997). Wall correction factor for sinking cylinders in fluids. *Physical Review E* (55), 2808.

Sugihara, M. and H. Niimi (1984). Asymmetric flow of a cylindrical particle through a narrow channel. *Journal of Applied Mechanics* (51), 879-884.

Tachibana, M. and Y. Iemoto (1987). Steady flow around, and drag on a circular cylinder moving at low speeds in a viscous liquid between two parallel planes. *Fluid Dynamics Research* (2), 125.

Takaisi, Y. (1955). The drag on a circular cylinder moving with low speeds in a viscous liquid between two parallel walls. *Journal of the Physical Society of Japan* (10), 685-693.

Takaisi, Y. (1956a). Note on the drag on a circular cylinder moving with low speeds in a viscous liquid between two parallel plane walls. *The Physical Society of Japan* (11), 1009-1013.

Takaisi, Y. (1956b). The drag on a circular cylinder placed in a stream of viscous liquid midway between two parallel plane walls. *Journal of the Physical Society of Japan* (11), 1092-1095.

Taneda, S. (1964). Experimental investigation of the wall-effect on a cylindrical obstacle moving in a viscous fluid at low Reynolds numbers. *Journal of the Physical Society of Japan* (19), 1024-1030.